ADVANCED MATERIALS TECHNOLOGIES
www.advmattechnol.de

Potential of Aluminum as a Metal Fuel for Supporting EU Long-Term Energy Storage Needs

Linda Barelli, Lorenzo Trombetti, Shuting Zhang, Hüseyin Ersoy, Manuel Baumann, and Stefano Passerini**

The EU's energy transition necessitates availability of green energy carriers with high volumetric energy densities for long-term energy storage (ES) needs. A fully decarbonized scenario considering renewable energy availability is analyzed underpinning the need for such carriers. Considering the shortcomings of Power-to-X technologies in terms of efficiency and low volumetric density, Aluminum (Al) is identified as a potential alternative showing significantly high volumetric energy densities (23.5 kWh L^{-1}). In this paper, an Al-based long-term ES concept is investigated, taking advantage of the inherent recycling of the active species (i.e., Al_2O_3 to Al) coupling decarbonized Hall–Héroult process with an Al-steam oxidation for simultaneous hydrogen (H_2) and heat generation. This work demonstrates an innovative lab-scale fine Al powder-steam oxidation process at ≈900 °C without use of catalysts or additives, exploiting alumina as inert material. Conducted SEM-EDX analysis on oxidized Al provides supporting evidence in favor of employed oxidation pathway, hindering tendency of aluminum oxide (Al_2O_3) clumping and enabling direct use of oxides in the smelting process for fully recyclability. Moreover, outcomes of XRD analyses are presented to validate the measured total H_2 yields.

1. Introduction

Long term energy storage (ES) to cope with the demand due to fluctuating behavior and seasonal variation of renewables is still a major challenge in frame of the energy transition. In line with this, H_2 is currently considered as one of the most promising energy carrier and storage medium to ensuring the availability of decarbonized energy supply on longer periods.[1] Furthermore, considering the required acceleration on implementation and adoption of green energy carriers for decarbonization of energy-intensive industry and long-distance transportation, availability of decarbonized/low-carbon H_2 still poses technological and supply chain related challenges. Improved conversion efficiency of electrolyzer and fuel cell technologies is a motivating aspect. Nevertheless, a significant amount of energy is lost during H_2 production and compression or liquefaction process. If the produced H_2 is converted into more volumetrically dense energy carriers such as ammonia, it provides improved techno-economics for transportation, but it needs to be cracked to H_2 gas requiring repetition of compression and liquefaction steps. This is also the case of methanol used as hydrogen carrier, which results in efficiency reduction of 12% with respect to compressed hydrogen (70 bar), in the power-to-power application employing a reversible solid oxide device.[2] An even greater efficiency reduction, resulting in 26.5% Round-Trip Efficiency (RTE), is foreseen if the required CO_2 is provided by direct air capture systems. Moreover, safety issues must be faced.

L. Barelli, L. Trombetti
Universitá Degli Studi Di Perugia (UNIPG)
Piazza dell'Università 1
Perugia 06123, Italy
E-mail: linda.barelli@unipg.it

S. Zhang, S. Passerini
Chemistry Department
Sapienza University of Rome
Piazzale A. Moro 5, Rome 00185, Italy
E-mail: stefano.passerini@kit.edu

The ORCID identification number(s) for the author(s) of this article can be found under https://doi.org/10.1002/admt.202302206

DOI: 10.1002/admt.202302206

H. Ersoy, M. Baumann, S. Passerini
Institute for Technology Assessment and System Analysis (ITAS)
Karlsruhe Institute of Technology (KIT)
Karlstraße 11, 76021 Karlsruhe, Germany

H. Ersoy
CENSE – Center for Environmental and Sustainability Research, NOVA School of Science and Technology
NOVA University Lisbon
Lisbon Portugal

S. Passerini
Helmholtz Institute Ulm for Electrochemical Energy Storage
Karlsruhe Institute of Technology (KIT)
Helmholtz Straße 11, 89081 Ulm, Germany

Considering all these energy-intensive process steps overall conversion efficiency declines further if H_2 is used for re-electrification showing 20–30% RTEs.[3] Supply chain related challenges are mainly associated with its transport and storage through supply chain as indicated in the IEA's "Global Hydrogen Review 2023".[4] Marine transportation and projected pipelines illustrate the main strategies for transportation and distribution of H_2 in Europe, however, storage of H_2 for bulk and long-term(duration) ES applications appears to be feasible only using underground storage, posing geographical constraints.[5] Use of existing natural gas storage infrastructure for H_2 storage is another consideration, nonetheless, available capacity by 2050 corresponds only to 10–25% of the needed H_2 according to IEA's Net Zero Emission (NZE) scenario.[6] Reflecting on advantages and disadvantages of H_2 as a green energy carrier, diversifying alternative energy carriers can be perceived as a complementary solution considering the required acceleration on decarbonization to stay in the limits of earth's carbon budget. Therefore, emerging concepts using metals as energy carriers for long-term(duration) energy storage demonstrate features to solve the challenges regarding volumetric energy density, material availability, ease of storage and transportation, as well as low cost and integration with industrial processes.[7,8]

Several reactive metals have been recently proposed by the authors,[2,9,10] highlighting Al, which is non-critical, non-toxic, and widely available, offering volumetric energy density of 23.5 kWh L^{-1}, RTEs competitive or even higher than H_2-based storage applications using low temperature electrolysis and fuel cells, and a fully circular process.[2] Model-based results show promising techno-economic feasibility and potentially improved environmental sustainability performance,[11–13] However, the absence of experimental demonstrations was previously identified as a research gap for such emerging concepts.

Specifically, while aluminum storage is inherently safe, ease to handle and it exhibits very high volumetric energy density, its conversion into hydrogen according to conventional processes presents some issues with respect to circularity and continuity of the process. As further detailed in Section 2, water oxidation needs additives (e.g., alkaline compounds) to promote the H_2 generation reaction. These additives could affect alumina reduction to aluminum in the Hall–Héroult process, unless additional treatments (e.g., water rinsing and subsequent calcination) are performed. On the other hand, steam combustion at temperatures above 1600 °C is affected by clogging issues generated by Al_2O_3 clumping. Thus, following the preliminary experimental demonstration of the process at intermediate temperatures (600–900 °C),[9] the feasibility of the process without technical impediments (clogging of the rector) and enabling the direct recycling of the produced Al_2O_3 in the Hall–Héroult process is a must be condition.

Accordingly, the flameless Al-steam oxidation process is experimentally assessed, aiming to address technical aspects beyond theoretical potential. As a novelty, this study presents the first experimental results proving feasible use of Al_2O_3 as inert material in the flameless Al-steam oxidation process at ≈900 °C. Such inert material prevents reactor clogging while enabling the fully recycling of produced powder in the Al smelting process without any preliminary treatment. The results provide supporting arguments about suitability of such a concept for continuous operating condition of a full-scale, fluidized-bed reactor, allowing to reduce of 2 orders of magnitude the required storage volume with respect to the case of underground H_2 storage. This outcome potentially contributes to solve H_2 storage issues and to expand green H_2 use in new applications, considering simultaneous H_2 and heat generation through steam Al oxidation. Finally, to assess the potential implementation scale of the proposed concept, the present study provides a quantitative assessment of the EU long-term storage capacity requirement for seasonal ES in the NZE scenario, as well as the impact of carriers' volumetric energy density on the required storage volume, assessing the benefit provided by aluminum exploitation.

2. Background: Aluminium-Steam Oxidation for Medium- and Long-Term Energy Storage

Herein, a circular seasonal ES concept is introduced employing round-trip conversion cycle (i.e., Power-to-Metal and Metal-to-X phases) over several different timescales (day-night to seasonal storage cycles) as illustrated in **Figure 1**. Considering that the concept employs 100% renewables for the Power-to-Metal path, up to 80% reduction in the associated GHG emissions can be foreseen considering the impact share of electricity on global warming potential of primary aluminum production.[14]

Excluding the pre-chain emissions (ideally the concept is circular, reducing the impacts on overall life cycle), a realistic decarbonization pathway can be assumed by elimination of direct emissions (i.e., CO_2 and fluorocarbon) thanks to inert anodes substituting conventional carbon anodes in the Hall–Héroult process.[15]

The Metal-to-X path is carried out using an innovative Al-steam oxidation process previously proposed and preliminary demonstrated experimentally.[9] The oxidation reaction shows variabilities depending on stoichiometric ratio of steam, and ambient conditions (e.g., pressure and temperature):

$$2Al + 6H_2O \rightarrow 2Al(OH)_3 + 3H_2 \qquad -886\ kJmol^{-1} \tag{1}$$

$$2Al + 4H_2O \rightarrow 2AlO(OH) + 3H_2 \qquad -862\ kJmol^{-1} \tag{2}$$

$$2Al + 3H_2O \rightarrow Al_2O_3 + 3H_2 \qquad -817\ kJmol^{-1} \tag{3}$$

Reactions 1 and 2 are typical of oxidation with water at low temperatures (below 300 °C). Although they grant the highest energy output, they have notable drawbacks tied to the need of additives in the water (e.g., alkaline compounds) to promote the H_2 generation reaction. Reaction 3 mechanism oxidizes Al in steam at temperatures above 1600 °C, but several issues arise due to the clumping of Al_2O_3.[16–19] Moreover, a previous study[9] proved the feasibility of Al oxidation in steam, according to Reaction 3, at temperatures ≈900 °C. Such innovative process at 800–1000 °C prevent the clumping of Al_2O_3 without requiring catalysts or additives. The obtained results (some details are summarized in *Test Procedure*) highlight that high conversion rates and long operating times are achievable by employing an inert material (perlite)

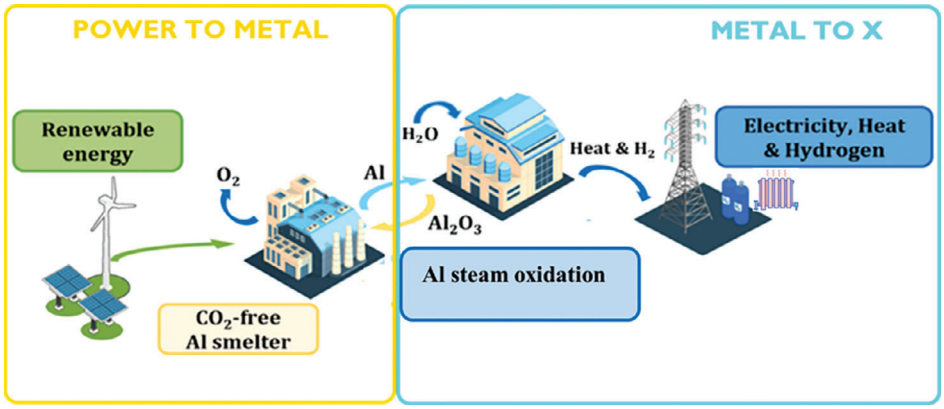

Figure 1. Schematic representation of the CO_2-free, fully circular, sustainable energy storage cycle based on Al.

to keep Al particles dispersed, preventing the clumping of Al oxide typical of vortex combustors.

3. Experimental Section

The approach in frame of this study is based on publications from the same authors' team. First, an Al-steam oxidation concept and a first 0-D model was developed.[2] This was followed by a comprehensive techno-economic assessment for different full load hours and multiple services of the same system.[13] Here the Al-steam combustion path is also compared to other long term storage alternatives. Then, a first sustainability screening of Al properties has been realized.[20] These studies provided promising results regarding technical as well as techno-economic performance and sustainability aspects (criticality, carbon footprint). Thus, in a further step, the demand for long-term storage that could be covered by the Al-steam oxidation is analyzed to understand the overall potential of the Al-steam oxidation concept. However, the named studies as well as the scenario assessment are based on theoretical assumptions, which must be proven. Consequently, after a preliminary experimental assessment,[9] the Al-steam oxidation is herein tested at the lab-scale to prove the technical feasibility of avoiding clogging of the rector and enabling the direct recycling of the produced Al_2O_3 in the Hall–Héroult process. This allows to derive major theoretical and experimental implications and to define next steps. The entire approach is provided in **Figure 2**.

3.1. Scenario-Based Assessment of European Long-Term Energy Storage Needs

This section is dedicated to the explorative investigation of the corresponding seasonal storage capacity needs based on NZE scenario by 2050. To do so, an hourly time series analysis has been conducted considering European energy generation mix based on historical data. The overall energy consumption was assumed to be equal to the European primary energy demand ($E_{p,d}$) recorded in 2018 (i.e., ≈21399 TWh).[21] Additionally, it was assumed that the primary energy needs would be fulfilled up to 90% with equal shares of wind and solar power.[22] Hence, analysis of PV and wind sources was performed over the generation data published by the European Network of Transmission System Operators for Electricity (ENTSO-E), which considers seasonal variations.[23] Based on this analysis the monthly fluctuation of PV and wind sources availability in different EU areas was assessed as detailed in the Supporting Information. Finally, the European ES demand has been estimated considering aggregated monthly generation profiles taking into account the following considerations:

1) Geographical distribution of conversion plants across Europe: according to,[24] wind energy generation in 2050 is expected to be predominant from latitudes of 45^0 N and higher, whereas PV installed generation capacity will prevail in the South area. Moreover, Centre and East areas were aggregated considering that i) only a limited number of countries are grouped in these areas according to the procedure detailed in the Supporting Information; ii) current reduced renewable production in East Europe (with respect to other EU areas) will have an effect on expected installed generation capacity in 2050. Wind and PV shares in the different areas are assumed equal to 0.55, 0.1, 0.35 and 0.35, 0.15, 0.5 for North, Centre and South areas, respectively.
2) Grid interconnection: it is assumed that the transnational grid will provide ("ideal" case) the full balancing across Europe between wind energy surplus from the Centre/North area and PV lack in the South during winter and vice versa in summer. It is highlighted as such an assumption will provide a minimum value of required EU long-term energy storage capacity. Consequently, the actual impact of green energy carriers' volumetric energy density might be greater than the one assessed according to this procedure.
3) Grid losses (ζ_G): the value of 5.8% is assumed based on the Italian grid losses given by Terna S.p.A., the Italian transmission system operator, for 2020.[25]
4) Energy storage round trip efficiency (RTE): 36% were assumed as indicated in ref. [11] for the Al-based energy storage cycle using an Al-steam oxidation. Notice, that his value is slightly greater than the one of H_2-based energy storage implementing low temperature electrolyzer and fuel cell technologies.

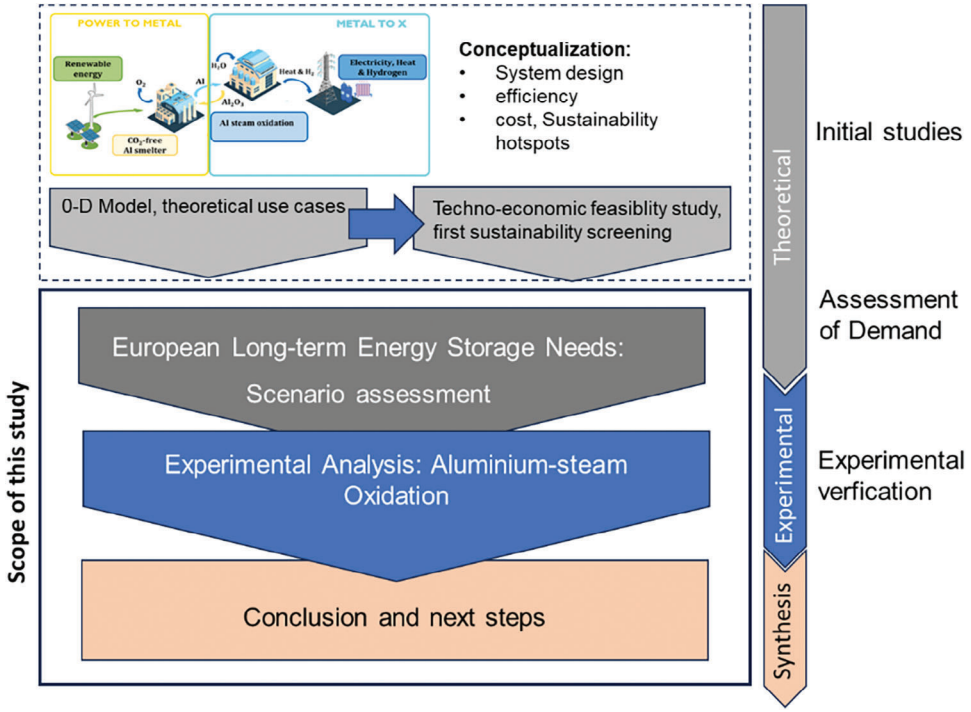

Figure 2. General approach starting from modeling and parametrization to experiments, and finally an explorative assessment on the demand for high density, long-term energy storage carriers.

Based on the last two assumptions, the primary energy demand is adjusted according to Equation 4 up to $E^*_{p,d} = 25128$ TWh, compensating for the storage efficiency and transmission losses. Consequently, an iterative procedure is implemented to assess $C_{S,tot}$ (where $C_{S,tot}$ $C_{S,tot}$is the seasonal energy storage capacity) $C_{S,tot}$once convergence is achieved.

$$E^*_{p,d} = \frac{E_{p,d} + (1 - RTE)\, C_{S,tot}/RTE}{1 - \zeta_G} \quad (4)$$

At each step moving from the current $C_{S,tot}$ value, $E^*_{p,d}$ is determined. $E^*_{p,d}$ is split according to 45–45% PV and wind shares. Then the resulting required generation capacities are further split by applying PV and wind shares previously assumed for the different EU areas. This results in the assessment of annual and monthly average generation per source and area. Based on these data the monthly generation profile per source is determined in the NZE scenario in each considered EU area (see Figure 4A discussed in next Section 4.1) using the monthly fluctuation of PV and wind sources availability previously determined (see Figure S1, Supporting Information).

Assuming the transnational grid to provide full balancing across Europe between surplus and deficit of renewable electricity generation in different areas, the overall renewable generation monthly trend is assessed. Finally, the trend of generation surplus/deficit can be computed with respect to the resulting average monthly generation capacity. With reference to Figure 4B (discussed in next Section 4.1), the integral of surplus (orange area) or deficit (blue area) along the year provides the $C_{S,tot}$ assessment to be considered in the next step up to convergence achievement.

3.2. Experimental Analysis: Aluminum-Steam Oxidation

3.2.1. Materials

The Al-steam oxidation was demonstrated using fixed bed reactors where the powder was kept pressed between two seals for simulating the favorable conditions for clogging. The tests were executed using two test benches. The first test bench (**Figure 3A**) included a vertical small capsule reactor with a reduced reaction zone of 140 mm length and 10 mm diameter, suitably developed for the preliminary investigation of the impact of alumina as the inert material on the Al oxidation. Accordingly, the second bench (Figure 3B) holded a larger tubular horizontal reactor (total length: 953 mm, external/internal diameter: 38.1/23.8 mm, isothermal zone: 476 mm) made of Hastelloy X for chemical, catalytic, and sorbing experiments operating at elevated temperatures (up to 900 °C) and pressure (up to 10 bars). Both the test benches enabled process control (regulating the reaction temperature and steam flow) delivering measurements for the generated H_2, as explained in Supporting Information (Section S2, Supporting Information).

Powder Preparation: Two Al powders were used, later named 120 mesh (particle diameter <125 µm, Goodfellow) and 325 mesh (particle diameter <44 µm, "Pure Al" from M4P).[26] The latter, being not a high purity Al powder, was chosen due to its commercial availability for industrial additive manufacturing applications. The Al powders were dispersed with various amounts of

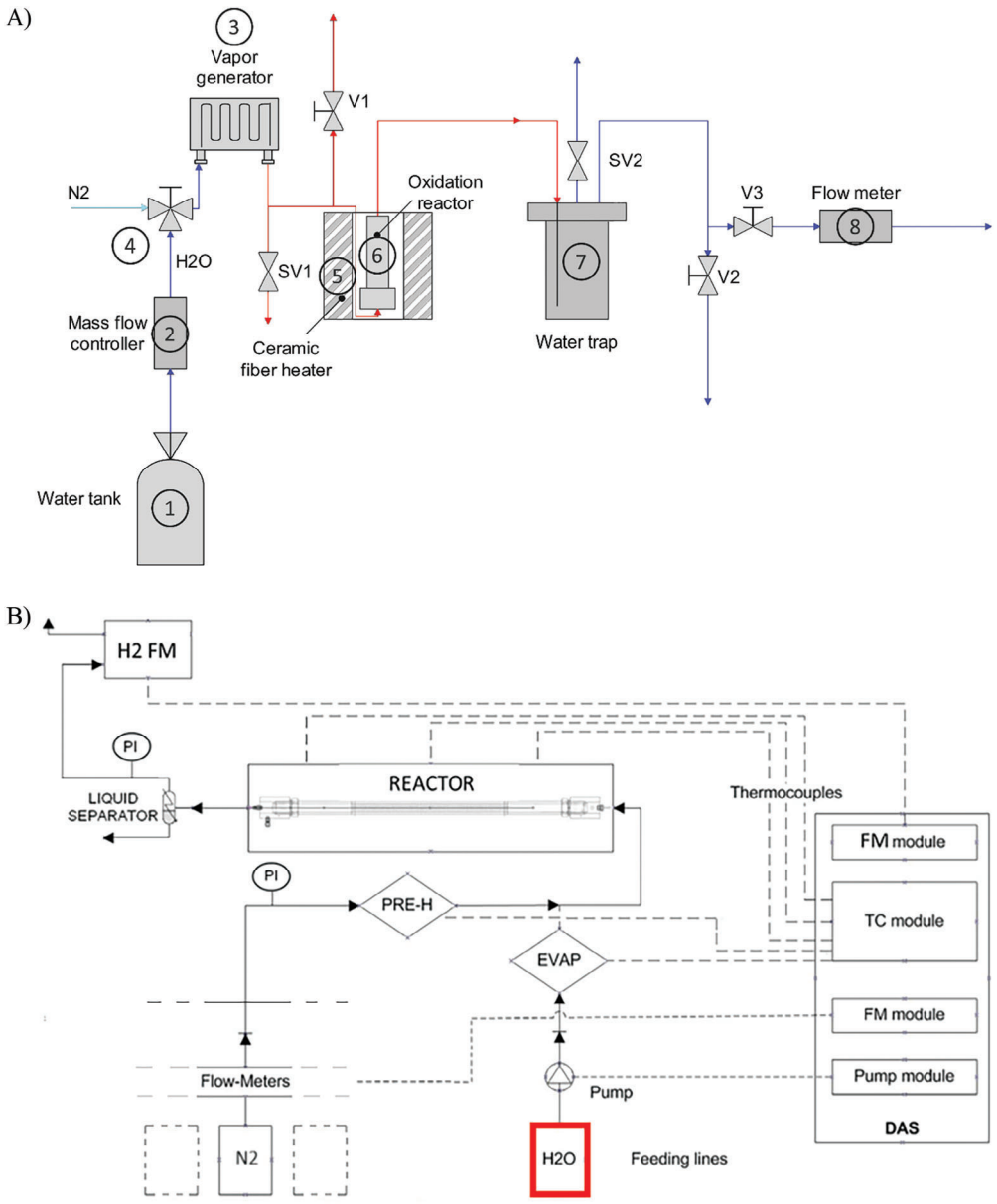

Figure 3. Layout of the test bench implementing A) the small vertical capsule reactor (reproduced from Ref. [9]. Copyright 2022, The Authors) and B) the large tubular reactor. All technical details are given in Supporting Information.

alumina (average particle size of 180 µm from Thermo Fisher Scientific) by manual mixing before being loaded into the selected test reactor. For the small test bench, glass wool fiber cylindrical plugs were used to immobilize the powder inside the reactor. These plugs were inserted into the reactor, one above and one below the loaded powder mixture. After sealing the reactor with its cap, it was pressurized to 3 bar to check for gas leaks. Subsequently, the reactor was connected to the test bench circuit and placed inside the ceramic heater.

The powder preparation for the large tubular reactor begins with the insertion of three plugs of glass wool with a diameter of 24 mm from the back end of the reactor. The plugs were pushed inside the reactor until they reach the middle section. The reactor was subsequently rotated vertically to allow the loading of the powder mixture. The remaining volume was filled with nine more glass wool plugs. To enhance the gas tightness of the system, a high-temperature, anti-seize paste was used to seal the inlet and outlet threaded caps of the reactor. Finally, the loaded reactor was connected to the test bench for testing.

3.2.2. Methods

Test Procedure: Before each test, the small and larger reactors were purged with nitrogen for 5 and 30 min, respectively, to prevent any undesired Al oxidation by exposure to remaining air. The reactors were heated accordingly to the chosen test temperature. Once the desired temperature for the experiment was attained in

Table 1. Al steam oxidation tests at 900 °C using alumina as inert material.

Test No	ID	Reactor	Temperature [°C]	Water Flow [g h^{-1}]	Al and Al_2O_3 quantity [g]	Al_2O_3 / Al	H_2O / Al [h^{-1}]	Al size [μm]
1	900-60-0.2A-125-0.4	Capsule reactor	900	60	0.2, 0.4	2	300	≤125
2	900-60-0.2A-125-0.8	Capsule reactor	900	60	0.2, 0.8	4	300	≤125
3	900-60-0.2A-44-0.8	Capsule reactor	900	60	0.2, 0.8	4	300	≤44
4	900-150-0.5A-44-2	Tubular reactor	900	150	0.5, 2	4	300	≤44

the reactor, a controlled stream of water was supplied to the steam generator. It is worth noting that the reaction was carried out under excess water to avoid limitation of the conversion reaction by water itself. As a result, the flow exiting the reactor consisted of a mixture of water and H_2. The excess water was condensed and separated in the dedicated sections of the test benches. The H_2 goes to the flow meter for the flow rate measurement. The flow of water was halted after 1 h for the capsule reactor and 2 h for the tubular reactor. After, the flow of H_2 gradually diminished, eventually reaching a complete halt within several minutes.

The total volume of H_2 (V_{H2}) produced during each test was determined through a multi-step process. First, the measured flow rate is integrated over the course of the entire test, which yields the total volume (V_{tot}) of gas recorded until the flow rate reached zero. This value was then adjusted by subtracting the initial volume of nitrogen (V_{in}) present at the beginning of the test and the volume of water (V_w) used during the test. The measured volume (V_{H2}) was converted to the mass of H_2 produced, considering its density at standard conditions (273.15 K and 1 atm). This allowed the assessment of the reacted Al mass ($m_{Al,\,R}$), as a complete Al conversion results in a H_2 production equivalent to 11.1% of the Al mass. The ratio between $m_{Al,\,R}$ and the initial mass of Al loaded into the reactor results in the Al conversion rate (%CR).

After the execution of each test the reactor was open and unloaded. Sample of the reaction products were collected and subjected to ex situ characterization by Scanning Electron Microscopy (SEM) equipped with an energy dispersive X-ray (EDX) detector and X-Ray Diffraction (XRD) measurements. The SEM-EDX images were obtained using a Zeiss CrossBeam XB340 microscope equipped with the Quantax 200 Bruker EDX. The XRD data were recorded on a Bruker Advance D8 diffractometer with Cu radiation ($Ka_{1,2}$ λ = 1.5406 Å, 1.5444 Å) in the 2θ range of 10–90°, with a step of 0.06° and a time per step of 3 s.

Test Campaign: The present work is built upon the previous experimental study of Al-steam oxidation, performed using an Al powder mixture (44 μm, Alfa Aesar) and granulated perlite (mm-scale), the latter acting as the inert.[9] The previous test campaigns were performed in 2 phases using the test rig of Figure 3A. The first phase focused on investigating the reaction of micron-sized Al at temperatures below (550–650 °C) and above (750–850 °C) the Al melting point, together with the effect of water flow rate and Al quantity on the H_2 production rate and total yield. The second phase was designed to focus entirely on the reaction at 900 °C, as the process temperature appeared to have the greatest effect on H_2 production. The results highlighted high Al conversion rates (%CR, defined as the mass ratio between reacted and inlet Al). Rietveld refinement was employed to assess the reaction yield based on the XRD pattern of the reaction product (test conditions 900-60-0.2P: 900 °C temperature, 60 g h^{-1} water flow rate, 0.2 g Al loaded quantity and 0.4 g loaded perlite) resulting in a predominant content of γ-Al_2O_3 (83.4%w). Furthermore, SEM and EDX analysis revealed as the process yielded to alumina (Al_2O_3) spherical microparticles mostly, which, together with the presence of inert perlite, avoided their coalescence, allowing 1 h operation without reactor clogging. The main outcomes have been reported in an early publication.[9]

The inclusion of perlite proved to be beneficial preventing the aggregation of Al particles and alumina, with particular attention to potential clogging effects during the conversion process. The test campaign performed in this study aimed at analyzing the effects of substituting granulated perlite with alumina powder with regards to the clogging tendency of the mixture in view of developing an innovative reactor technology for continuous steam oxidation. In fact, the simple and low-cost integration of the Metal-to-X with the Power-to-Metal conversion paths (CO_2-free Hall–Héroult process) requires alumina and unreacted Al to be the only solid components coming out of the Al steam oxidation reactor.

Experimental Tests in the Small Capsule Reactor: A series of preliminary tests were conducted at 900 °C with a steam flow rate of 60 g h^{-1} and Al quantity of 0.2 g based on the previous results. With reference to the previously performed tests,[9] the main difference lies in the variable quantity of inert alumina replacing perlite. Additionally, the tests were performed also using a different Al powder with a rather lower mesh than the previously employed powder (125 μm vs 44 μm). The first test was carried out by substituting perlite with the same mass of alumina (0.4 g). In the second test, the amount of alumina was increased to four times the Al powder mass (0.8 g). The last test was instead carried out with the same ratio of powders but using the Al powder with a maximum diameter of 44 μm.

Experimental Tests on the Large Tubular Reactor: Multiple tests were performed on the larger reactor at 900 °C using the same steam flow rate to Al weight ratio and Al to Al_2O_3 weight ratio of test 900-60-0.2P. The operating conditions investigated on both test benches are summarized in **Table 1**.

3.2.3. Statistical Analysis

The Al-steam oxidation experiments were repeated varying several parameters as indicated in Table 1. Since the equipment was in-house made and the distribution of the loaded sample in the reactor not very reproducible, an accurate statistical analysis is not feasible. However, the reactors were calibrated according to the procedure described in ref. [9]. The XRD and EDX

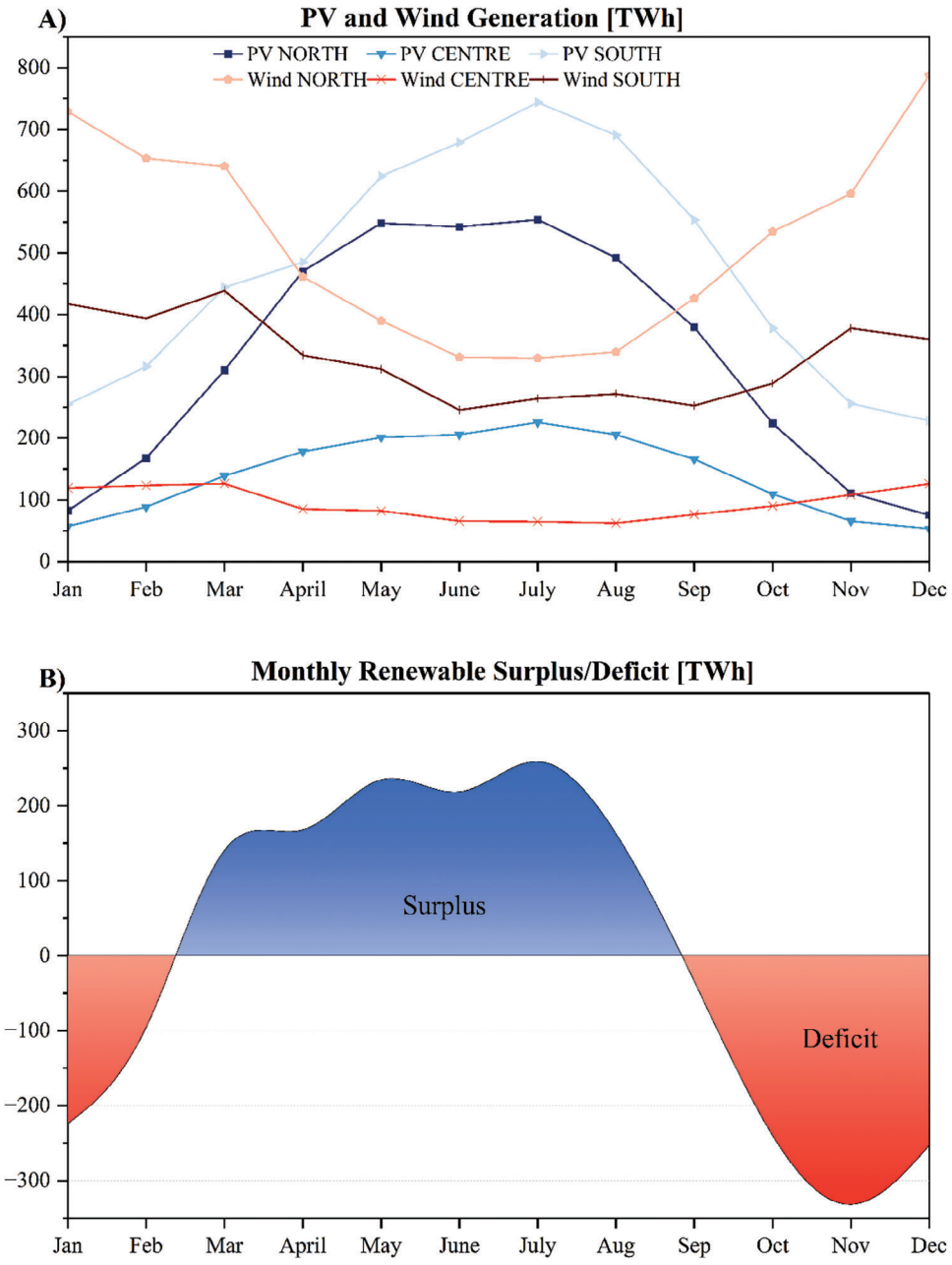

Figure 4. A) Monthly profiles of wind and PV generation assessed in the NZE 2050 scenario. B) Overall renewable generation surplus/deficit monthly trends.

measurements and SEM images were taken in several different portions of the collected samples. Only the most occurring results are reported herein.

4. Results

4.1. Scenario-Based Seasonal Volumetric Energy Storage Requirements

As mentioned before, the Al-steam oxidation shows promising theoretical results for long-term energy storage, considering some preconditions (e.g., circularity of the Al, use of renewables). Details on the theoretical techno-economic performance of the system and the sustainability of Al can be found in,[2,9,20] The remaining question though, is if there is the demand for this kind of seasonal energy storage solution, and where it is required. Bearing that in mind, seasonal and geographical variabilities of solar and wind power generation are considered with respect to the corresponding annual average values separately for Northern, Central, Eastern, and Southern Europe. The resulting trend illustrated in Figure S1 (Supporting Information) implies opposite seasonal trends for wind and solar generation, proving that they

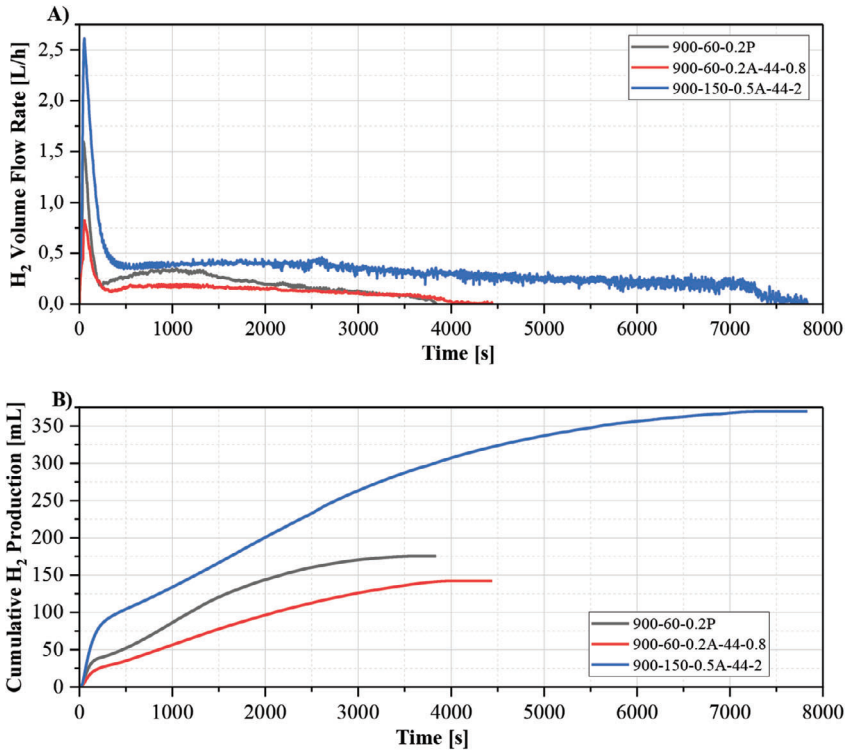

Figure 5. A) H2 volume flow rate obtained during tests 900-60-0.2A-44-0.8 and 900-150-0.5A-44-2. For the sake of comparison, the result of a previously reported test 900-60-0.2P is also illustrated (data taken from ref. [9]. Copyright 2022, The Authors). B) Cumulative H_2 production curves for tests 900-60-0.2A-44-0.8, 900-150-0.5A-44-2 and 900-60-0.2P.

can only partially compensate each other due to their different shares in the generation mix of various European regions. Ideally, the deficit in the renewable energy supply is stored via the use of long-term/seasonal ES.

The estimated monthly generation profile per source and region in accordance with the NZE scenario in 2050, determined under the methodology and assumptions stated in the previous Section 3.1, is illustrated in **Figure** 4A. Based on that, the overall monthly renewable generation trend is derived. It must be highlighted that the shown approach allows the minimization of installed wind and PV plants, since installed power is sized to provide a generation capacity close to the primary energy need, while seasonal storage allows to overcome temporal gaps.

With respect to the resulting average monthly generation capacity, the trend of generation surplus/deficit is analyzed (Figure 4B) and an annual ES capacity of 1278 TWh is estimated. Considering the Al volumetric energy density (23.5 kWh L^{-1}) a storage volume of ≈54.4 Mm^3 is estimated to satisfy the seasonal deficit in renewable energy supply. From a practical point of view, the needed storage volume corresponds to only ≈46 soccer fields covered with 7 meters of Al.

According to the "Fuel Cells and Hydrogen 2 Joint Undertaking in the Hydrogen Roadmap Europe" estimations,[27] exploiting H_2 as the intersectoral energy carrier requires the generation of ≈2250 TWh, thereof 1451 TWh to satisfy transportation, heating and power for buildings and energy for industry demands in the decarbonized 2050 scenario. This is the amount to be considered since it refers to the primary energy consumption $E_{p,d}E_{p,d}$. Furthermore 112 TWh for short-term grid services as well as 391 TWh and 257 TWh for existent and new industrial feedstocks (mostly in the refining and chemical production industries) are assessed, which is out the scope of this study. Thus, considering H_2 as a main energy carrier, the implemented method results in 1322 TWh. Such a value of long-term energy storage capacity is assessed considering a H_2-based energy storage cycle integrating alkaline water electrolyzer, PEM fuel cell stacks, and H_2 storage at 700 bars with 30% RTE. Assumptions made to support the chosen RTE value are detailed in the Supporting Information (Section S3, Supporting Information). With such an energy carrier, the storage volume increases up to ≈944 Mm^3 mainly as consequence of its low volumetric energy density (1.4 kWh L^{-1}). Even worse, for the first storage demonstrator of green H_2 in salt cavern operating at 130 bars,[28] the volumetric energy density further diminishes to ≈0.33 kWh L^{-1}, increasing the storage volume required at the European level up to 3900 Mm^3. Such a volume is further increased since an internal minimum pressure of 110 bar must be maintained.

4.2. Experimental Results: Al-Steam Oxidation

The first two tests (Test 1 (Test ID: 900-60-0.2A-125-0.4) and Test 2 (Test ID: 900-60-0.2A-125-0.8) see Table 1), employing the 125 mesh Al powder and executed in the small capsule reactor, did not run to completion. Test 1 started with an unstable water flow rate caused by the reactor's clogging, which

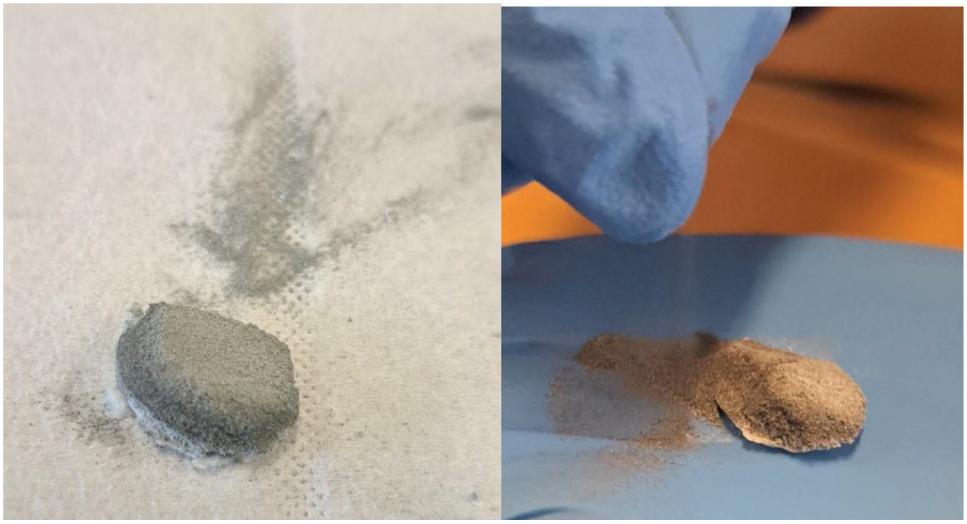

Figure 6. Appearance of the powder resulting from the steam oxidation process (Test 4).

resulted in the complete halt after 15 min. Test 2 ran for 30 min before halting for the reactor clogging. Therefore, a third test (Test 3, Test ID: 900-60-0.2A-44-0.8, red curve in Figure 4) was executed using the small reactor, but using the 325 mesh Al powder, which ran to completion. For the sake of comparison, the H_2 generation rate from a previously conducted test is also reported in the figure (Test ID: 900-60-0.2P, gray curve in **Figure** 5A). As expected, Test 3 showed a lower H_2 production rate with respect to the previous report, due to the different type and purity of Al, and a slightly reduced cumulative H_2 production (from 175.5 to 142.2 mL, as illustrated in Figure 5B). Additionally, the H_2 production profile had a regular trend, i.e., no steep H_2 flow variations ascribable to clogging and unclogging of the reactor, supporting for the formation of small Al_2O_3 particles, as confirmed by the SEM analysis presented later in Section 4.2.1.

Following these positive results, the process was further investigated using the large tubular reactor under the same operating conditions, but the uploaded amount of Al was increased to 0.5 g as indicated in Table 1. The H_2 production rate of Test 4 (Test ID: 900-150-0.5A-44-2; blue curve in Figure 5A) is characterized by a higher initial peak and longer duration, but with a similar profile to Test 3. Also, the observed total H_2 yield (369.3 mL) is slightly greater than that obtained in Test 3, especially considering the 2.5-fold increase in the Al mass.

Once more, the H_2 flow rate profile confirms the absence of clogging effects. The collected powder appeared as a macroaggregate (**Figure 6**, picture on the left-hand side), which crumbles into extremely fine dust as soon as it is touched (Figure 6, picture on the right-hand side). This proves the effectiveness of using alumina as inert material in the steam oxidation process of fine (325 mesh) Al powder.

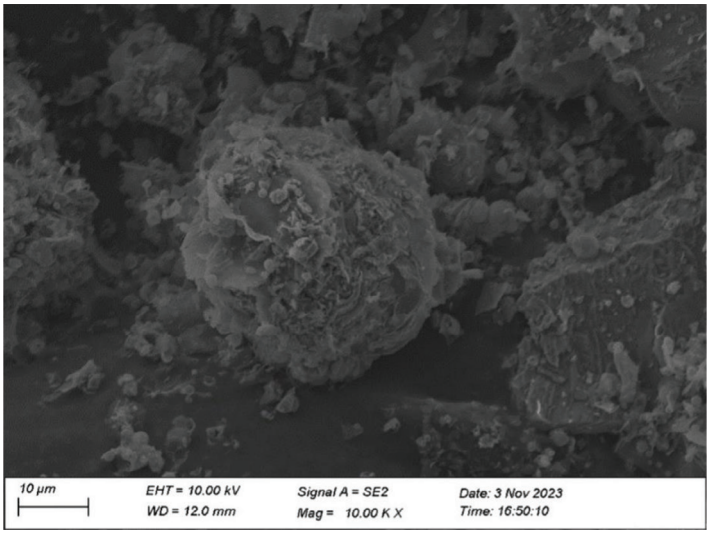

Figure 7. SEM image of a reacted Al particle after steam oxidation (Test 4).

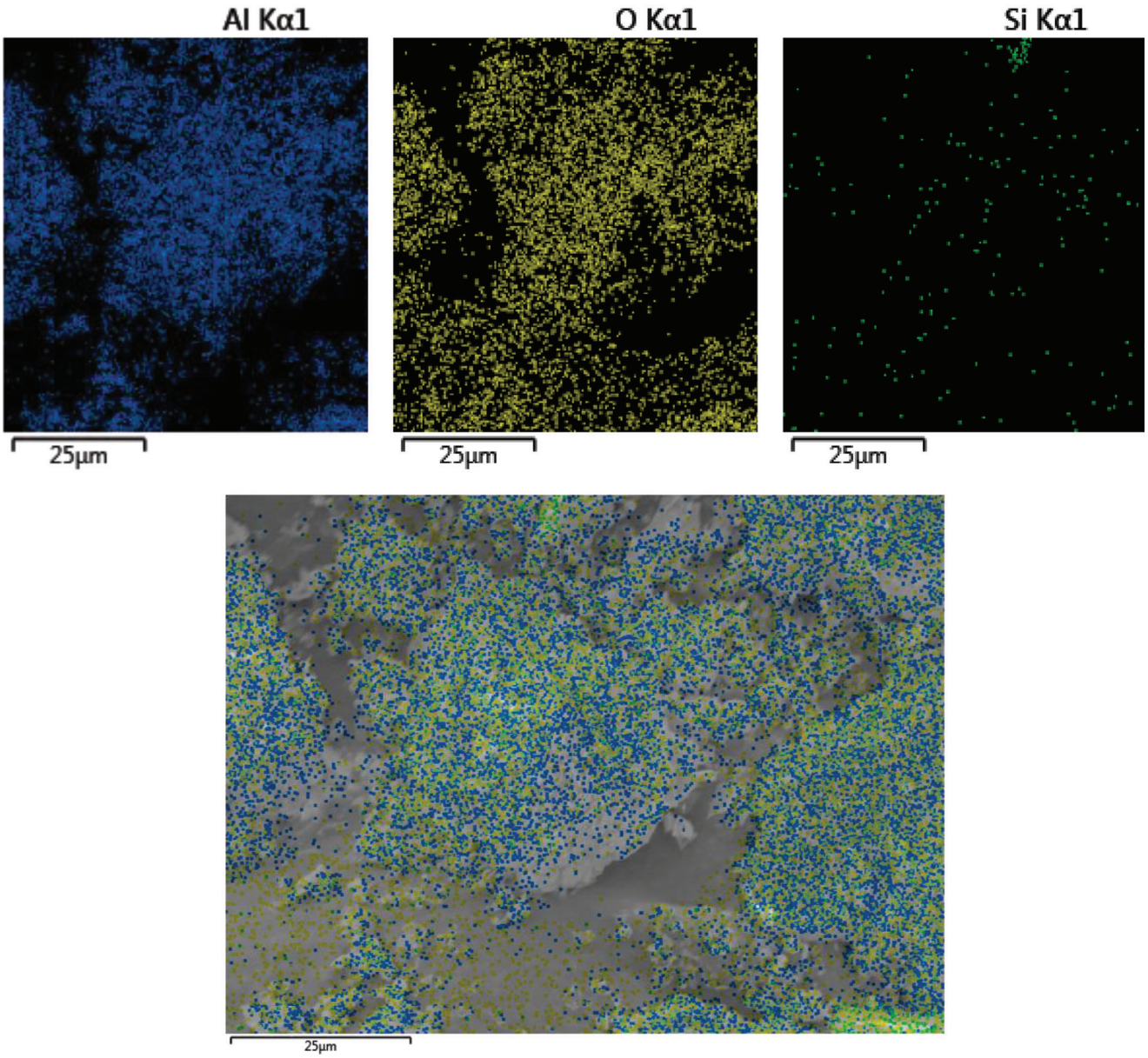

Figure 8. EDX mapping of a reacted Al particle after steam oxidation (Test 4).

4.2.1. Characterization of Al-Steam Reaction Products

The materials collected after Test 3 and Test 4 were further investigated via ex situ SEM-EDX and XRD analyses and compared with the 325 mesh Al powder as well as the alumina powders used as inert. Since rather similar results were found for the materials resulting from the two tests cited above, only the measurements made on the powder collected after the Test 4 are presented, while the results for the powder collected from Test 3 and the reference materials are reported in Supporting Information (Figures S2–S5, Supporting Information).

Figure 7 depicts a 10 kX SEM image made pointing at a reacted Al particle. If compared with the SEM image of the 325 mesh Al (see Figure S4, Supporting Information), microparticle exfoliation is observed. After steam oxidation the surface of the particle is coated with tiny flake-like and spherical Al_2O_3 particles, as resulting from EDX analysis reported in **Figure 8**, similarly to the results reported when perlite was used[9] thus confirming the formation of alumina. Similar results were found for the material resulting from the Test 3 as evident from Figures S2 and S3 (Supporting Information) and their comparison with Figures 7 and 8. With reference to Figure 8, the observed presence of Si is clearly due to the glass wool fiber used to pack the Al powder in the reactor.

The 325 mesh Al powder is composed of smooth spheres, as depicted in Figure S4 (Supporting Information). Upon steam oxidation reaction, the Al spheres revealed a composite nature, comprising Al_2O_3, unreacted Al, and SiO_2 (from the glass wool fiber)

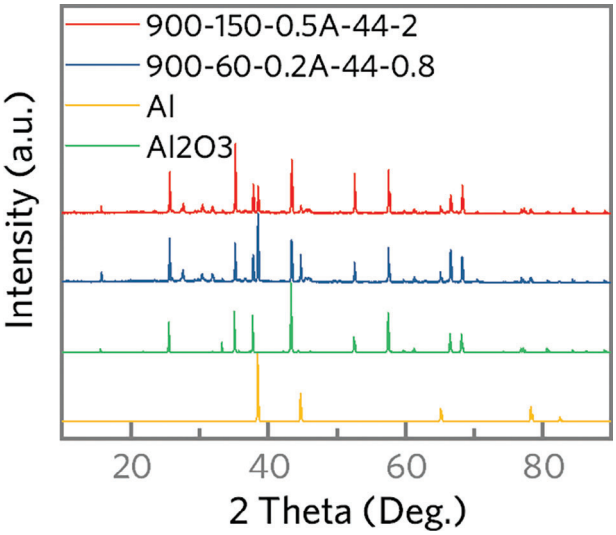

Figure 9. XRD patterns of reacted Al particles after steam oxidation (Test 3 and Test 4). For comparison, the patterns of 325 mesh Al as well as inert alumina are also reported.

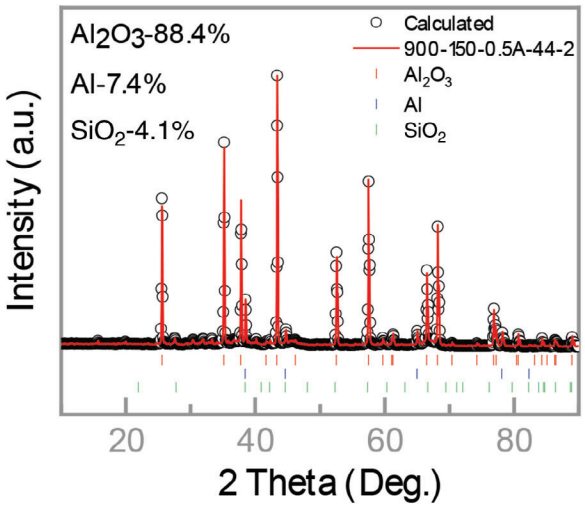

Figure 10. Quantification of the reacted Al powder composition after steam oxidation (Test 4) performed by Rietveld phase fraction analysis utilizing Highscore software.

as indicated by SEM and EDX analysis illustrated in Figures 7 and 8. Nonetheless, Figure 7 shows that the Al spheres remained intact, i.e., without merging, despite the reaction temperature being higher than the Al melting point. This certainly results from the formation of the Al_2O_3 shell encasing molten Al. The surface of the sphere revealed a laminar structure, but also small spherical Al_2O_3 particles corresponding to a partial leaking of molten Al.

XRD analysis was also performed to assess the extent of oxidation within the bulk of Al particles, using as reference both the inert alumina and the 325 mesh Al powder.

Figure 9 presents the XRD patterns of the materials collected after Test 3 and Test 4. Both samples exhibited the presence of Al and Al_2O_3, further validating the EDX analysis (Figure 8). However, the Al peaks appear to be weaker in the material resulting from the Test 4, implying a higher conversion rate in the large reactor. To gain further insights into the conversion rate during the Test 4, the Rietveld phase fraction analysis[29] utilizing High score software, was applied. As reported in **Figure 10**, the analysis unveiled an 88.4% fraction of Al_2O_3, while Al exhibited a significantly lower fraction of 7.4%.

These outcomes are consistent with the results obtained in terms of H_2 production. In **Table 2** the residual Al content is assessed at 7.2% considering the H_2 total yield of 369.3 mL which corresponds to %CR of ≈60% (i.e., 0.3 g of reacted Al over 0.5 g initially loaded in the reactor). Also, the mass of alumina (2 g) initially loaded in the reactor is considered.

5. Conclusion

The goal of the study is to fill the gaps remaining from the previous theoretical technical and technoeconomic feasibility studies, namely, the demand for the proposed seasonal energy storage alternatives in Europe and the experimental validation of the Al-steam oxidation concept. Consequently, the seasonal storage demand at the EU level was assessed to overcome temporal gaps of renewable generation, optimizing wind and PV installed power capacity to provide a generation capacity close to the primary energy need. Identifying the volumetric long-term ES needs in terms of seasonal storage and assessing technical advantages that aluminum as an energy carrier can provide are the important outcomes of the conducted study. The long-term ES demand analysis in frame of the scenario analysis provides arguments in favor of a diversification of storage options, since projected H_2 requirements, volumetric needs, and geographical as well as geopolitical concerns are highly associated with this strategy. A fully decarbonized scenario requires the availability of 1278 TWh long-term ES capacities, considering the implementation at systemic level of the carbon-free energy storage circle based on Al as storage medium. Whereas, more than ≈70 times higher volumes will be required for H_2 (considering typical underground H_2 storage conditions). Storing renewable in stable, solid energy carriers in addition to volumetric advantages bring along benefits in terms of transportation, which poses challenges for other storage media. The corresponding quantity of Al to be produced on yearly base to guarantee the EU energy security by 2050, is assessed at ≈147 Mt (or 54.4 Mm^3), without a related consumption of raw materials thanks to the inherent recycling provided by the proposed energy storage circle. Anyway, a huge increase in the installation of Al smelting plants is required, being a motivating

Table 2. Assessment of produced powder composition based on measured H_2 total yield.

	Mass (g)	%w
Produced Al_2O_3	0.5667	20.5%
Initial inert Al_2O_3	2	72.3%
Total Al_2O_3	2.5667	92.8%
residual Al	0.2	7.2%
Total powder mass	2.7667	

aspect based on the potential techno-economic, social, and environmental benefits.

The proposed concept uses conventional process equipment that is indeed not very much different than a co-generation plant except the steam combustion chamber. Nevertheless, a step further has been taken in this work by consideration of Al_2O_3 as an inert material. Specifically, the demonstration and executed tests revealed that Al oxidation is enabled using Al_2O_3 itself as inert, which eliminates the concerns regarding effective circularity of the concept. Hence, the presented perspective with the scenario-based analysis is brought together with feasibility of the concept in this paper for supporting its further consideration.

Finally, the development of a suitable reactor architecture at the full-scale will be addressed in the next future to guarantee a continuous process. In line with that, further studies for economic feasibility and sustainability aspects will be carried out in parallel.

Supporting Information

Supporting Information is available from the Wiley Online Library or from the author.

Acknowledgements

S.Z. gratefully thanks the support fellowship of the Chinese Scholarship Council (CSC). S.P. and S.Z. acknowledge the support of the Helmholtz Association. All authors acknowledge the support of the European Commission under the project StoRIES (GAP-101036910).

Open access funding enabled and organized by Projekt DEAL.

Conflict of Interest

The authors declare no conflict of interest.

Data Availability Statement

The data that support the findings of this study are available on request from the corresponding author. The data are not publicly available due to privacy or ethical restrictions.

Keywords

aluminum steam oxidation, green energy carriers, hydrogen generation, seasonal energy storage

Received: December 21, 2023
Revised: April 20, 2024
Published online:

[1] T. Capurso, M. Stefanizzi, M. Torresi, S. M. Camporeale, *Energy Convers. Manage.* **2022**, *251*, 114898.
[2] L. Barelli, M. Baumann, G. Bidini, P. A. Ottaviano, R. V. Schneider, S. Passerini, L. Trombetti, *Energy Technol.* **2020**, *8*, 2000233.
[3] A. Escamilla, D. Sánchez, L. García-Rodríguez, *Int. J. Hydrogen Energy* **2022**, *47*, 17505.
[4] IEA, "Global Hydrogen Review 2023 – Analysis," IEA, https://www.iea.org/reports/global-hydrogen-review-2023, (accessed: December 2023).
[5] R. Tarkowski, B. Uliasz-Misiak, *Renewable Sustainable Energy Rev.* **2022**, *162*, 112451.
[6] IEA, "World Energy Outlook 2022," **2022**.
[7] M. Y. Haller, D. Carbonell, M. Dudita, D. Zenhäusern, A. Häberle, *Energy Conversion and Management: X* **2020**, *5*, 100017.
[8] K. A. Trowell, S. Goroshin, D. L. Frost, J. M. Bergthorson, *Appl. Energy* **2020**, *275*, 115112.
[9] L. Barelli, L. Trombetti, A. Di Michele, L. Gammaitoni, J. Asenbauer, S. Passerini, *Energy Tech.* **2022**, *10*, 2200441.
[10] M. Baumann, L. Barelli, S. Passerini, *Adv. Energy Mater.* **2020**, *10*, 2001002.
[11] J. M. Bergthorson, *Prog. Energy Combust. Sci.* **2018**, *68*, 169.
[12] M. Pini, G. Breglia, M. Venturelli, L. Montorsi, M. Milani, P. Neri, A. M. Ferrari, *Renewable Energy* **2020**, *154*, 532.
[13] H. Ersoy, M. Baumann, L. Barelli, A. Ottaviano, L. Trombetti, M. Weil, S. Passerini, *Adv. Mater. Technol.* **2022**, *7*, 2101400.
[14] P. Nunez, S. Jones, *Int. J. Life Cycle Assess* **2016**, *21*, 1594.
[15] ELYSIS, "Rio Tinto and Alcoa announce world's first carbon-free aluminium smelting process," ELYSIS, https://www.elysis.com/en/rio-tinto-and-alcoa-announce-worlds-first-carbon-free-aluminium-smelting-process, (accessed: March 2021).
[16] J. Foote, J. Lineberry, B. Thompson, B. Winkelman, in 32nd Joint Propulsion Conf. and Exhibit, American Institute of Aeronautics and Astronautics, Lake Buena Vista, FL, USA **1996**.
[17] T. F. Miller, J. L. Walter, D. H. Kiely, in Proc. of the 2002 Workshop on Autonomous Underwater Vehicles, IEEE, San Antonio, TX, USA **2002**, 111.
[18] X. Chen, Z. Xia, L. Huang, X. Na, J. Hu, *Energy Fuels* **2018**, *32*, 2458.
[19] X. Chen, Z. Xia, L. Huang, L. Ma, *Energies* **2016**, *9*, 1072.
[20] H. Ersoy, M. Baumann, M. Weil, L. Barelli, S. Passerini, in *Sustainable Energy Storage in the Scope of Circular Economy*, 1st ed., (Eds: C. M. Costa, R. Gonçalves, S. Lanceros-Méndez), Wiley, Hoboken, NJ **2023**, 17.
[21] "World Energy Consumption Statistics | Enerdata.", https://yearbook.enerdata.net/total-energy/world-consumption-statistics.html, (accessed: December 2023).
[22] European Commission. Joint Research Centre., Towards net-zero emissions in the EU energy system by 2050: insights from scenarios in line with the 2030 and 2050 ambitions of the European Green Deal, LU: Publications Office, 2023, https://data.europa.eu/doi/10.2760/081488, (accessed: December 2023).
[23] "ENTSO-E Transparency Platform.", https://transparency.entsoe.eu/dashboard/show, (accessed: December 2023).
[24] D. Bogdanov, M. Ram, A. Aghahosseini, A. Gulagi, A. S. Oyewo, M. Child, U. Caldera, K. Sadovskaia, J. Farfan, L. De Souza Noel Simas Barbosa, M. Fasihi, S. Khalili, T. Traber, C. Breyer, *Energy* **2021**, *227*, 120467.
[25] Terna S.p.A., "Popolazione, reddito e consumi energetici in Italia", https://download.terna.it/terna/0000/1089/73.PDF, (accessed: January 2024).
[26] metals4printing, "m4p PureAl – Technical Datasheet", https://www.metals4printing.com/wp-content/uploads/2021/Data_Sheets/EN/04_m4p_DataSheet_PureAl_EN.pdf, (accessed: January 2024).
[27] Fuel Cells and Hydrogen 2 Joint Undertaking., Hydrogen roadmap Europe :a sustainable pathway for the European energy transition. LU: Publications Office, 2016, https://data.europa.eu/doi/10.2843/249013, (accessed: April 2022).
[28] "About the Project | HyPSTER", https://hypster-project.eu/about-the-project/ (accessed: December 2023).
[29] I. C. Madsen, N. V. Y. Scarlett, L. M. D. Cranswick, T. Lwin, *J. Appl. Crystallogr. 34*, 409.